






Article

Pressure Tuning of Superconductivity of LaPt₄Ge₁₂ and PrPt₄Ge₁₂ Single Crystals

Gustavo A. Lombardi ¹, Kamal Mydeen ², Roman Gumeniuk ^{2,3}, Andreas Leithe-Jasper ², Walter Schnelle ², Ricardo D. dos Reis ¹ and Michael Nicklas ^{2,*}

- ¹ Brazilian Synchrotron Light Laboratory (LNLS), Brazilian Center for Research in Energy and Materials (CNPEM), Campinas 13083-970, SP, Brazil; gustavo.lombardi@lnls.br (G.A.L.); ricardo.reis@lnls.br (R.D.d.R.)
- ² Max Planck Institute for Chemical Physics of Solids, Nöthnitzer Str. 40, 01187 Dresden, Germany; kmydeenhp@gmail.com (K.M.); andreas.leithe-jasper@cpfs.mpg.de (A.L.-J.); walter.schnelle@cpfs.mpg.de (W.S.)
- ³ Institut für Experimentelle Physik, TU Bergakademie Freiberg, Leipziger Straße 23, 09596 Freiberg, Germany; roman.gumeniuk@physik.tu-freiberg.de
- * Correspondence: michael.nicklas@cpfs.mpg.de

Abstract: We carried out electrical resistivity and X-ray diffraction (XRD) studies on the filled skutterudite superconductors LaPt₄Ge₁₂ and PrPt₄Ge₁₂ under hydrostatic pressure. The superconducting transition temperature T_c is linearly suppressed upon increasing pressure, though the effect of pressure on T_c is rather weak. From the analysis of the XRD data, we obtain bulk moduli of $B = 106$ GPa and $B = 83$ GPa for LaPt₄Ge₁₂ and PrPt₄Ge₁₂, respectively. The knowledge of the bulk modulus allows us to compare the dependence of T_c on the unit-cell volume from our pressure study directly with that found in the substitution series La_{1-x}Pr_xPt₄Ge₁₂. We find that application of hydrostatic pressure can be characterized mainly as a volume effect in LaPt₄Ge₁₂ and PrPt₄Ge₁₂, while substitution of Pr for La in La_{1-x}Pr_xPt₄Ge₁₂ yields features going beyond a simple picture.

Keywords: superconductivity; hydrostatic pressure; bulk modulus; skutterudites



Citation: Lombardi, G.A.; Mydeen, K.; Gumeniuk, R.; Leithe-Jasper, A.; Schnelle, W.; dos Reis, R.D.; Nicklas, M. Pressure Tuning of Superconductivity of LaPt₄Ge₁₂ and PrPt₄Ge₁₂ Single Crystals. *Materials* **2022**, *15*, 2743. <https://doi.org/10.3390/ma15082743>

Academic Editor: Yong Seung Kwon

Received: 22 March 2022

Accepted: 7 April 2022

Published: 8 April 2022

Publisher's Note: MDPI stays neutral with regard to jurisdictional claims in published maps and institutional affiliations.



Copyright: © 2022 by the authors. Licensee MDPI, Basel, Switzerland. This article is an open access article distributed under the terms and conditions of the Creative Commons Attribution (CC BY) license (<https://creativecommons.org/licenses/by/4.0/>).

1. Introduction

The family of filled skutterudite compounds MPt₄Ge₁₂ crystallizes in the cubic LaFe₄P₁₂-type structure [1]. Depending on the filler metal ions M a variety of different ground states has been reported. The Pt–Ge framework is capable of incorporating the alkaline-earth metals Sr and Ba [2,3] rare-earth metals La, Ce, Pr, Nd, Sm, and Eu [3] as well as the actinides Th [4] and U [5].

NdPt₄Ge₁₂ and EuPt₄Ge₁₂ display complex magnetic phase diagrams at low temperatures [6], SmPt₄Ge₁₂ is an intermediate valence compound not showing any ordering phenomena [7,8] and CePt₄Ge₁₂ sits at the border between intermediate valence of Ce and heavy-fermion behavior [8–11]. Finally, several MPt₄Ge₁₂ compounds ($M = \text{Sr, Ba, La, Pr, Th}$) become superconductors with T_c up to 8.3 K [2,3,5].

The two superconducting family members LaPt₄Ge₁₂ and PrPt₄Ge₁₂, with T_c of 8.3 K and 7.9 K, respectively [3], have drawn a lot of attention due to their relatively high T_c and their unusual superconducting properties. It is important to note that the Pr ion is in a singlet crystalline electric field ground state in PrPt₄Ge₁₂ and therefore nonmagnetic at low temperatures [3,12].

The nature of the superconducting order parameter in LaPt₄Ge₁₂ and PrPt₄Ge₁₂ is still under debate. In PrPt₄Ge₁₂, there are indications for the presence of point nodes in the superconducting energy-gap function from nuclear magnetic resonance (NMR) [13], specific heat and penetration depth [14] measurements. Furthermore, several physical probes suggest the multi-band character of superconductivity in PrPt₄Ge₁₂ [14–22]. Moreover, there is convincing evidence for time-reversal-symmetry breaking superconductivity in PrPt₄Ge₁₂ provided by muon-spin-rotation (μ SR) experiments [12,23–25].

In $\text{LaPt}_4\text{Ge}_{12}$, the situation concerning the nature of the superconducting gap is less clear than in $\text{PrPt}_4\text{Ge}_{12}$. There is evidence for a single isotropic gap from specific heat and thermal conductivity [26], NMR [9], and photoelectron spectroscopy [15], while other studies using specific heat [19], μSR and penetration-depth measurements [27], and Fermi-surface studies [22] point at a multi-gap superconducting order parameter.

In contrast, the continuous evolution of the superconducting T_c along the substitution series $\text{La}_{1-x}\text{Pr}_x\text{Pt}_4\text{Ge}_{12}$ suggests compatible order parameters of both series end compounds [12,25]. Indications for time-reversal symmetry breaking are absent in $\text{LaPt}_4\text{Ge}_{12}$ [12], but they are observed for Pr concentrations $x \gtrsim 0.5$ in $\text{La}_{1-x}\text{Pr}_x\text{Pt}_4\text{Ge}_{12}$ [25]. What remains unclear is the origin of the pronounced minimum in $T_c(x)$ around $x \approx 0.75$ [12,25]. Its position does not seem to be related with the observation of the time-reversal symmetry breaking superconductivity. In contrast to $T_c(x)$, the unit-cell volume decreases monotonously with increasing x in the series in $\text{La}_{1-x}\text{Pr}_x\text{Pt}_4\text{Ge}_{12}$. This calls for hydrostatic pressure experiments on $\text{LaPt}_4\text{Ge}_{12}$ and $\text{PrPt}_4\text{Ge}_{12}$ to investigate the effect of a change in the unit-cell volume on the superconducting properties avoiding the complications of chemical substitution.

In the present paper, we performed an electrical resistivity and X-ray diffraction (XRD) study under hydrostatic pressure on $\text{LaPt}_4\text{Ge}_{12}$ and $\text{PrPt}_4\text{Ge}_{12}$. By combining the results from both experiments we obtain the dependence of the superconducting transition temperature on the unit-cell volume V of the cubic crystal structure for both compounds. This allows us to compare directly the effect of hydrostatic pressure on superconductivity in the end member compounds with that in the substitution series $\text{La}_{1-x}\text{Pr}_x\text{Pt}_4\text{Ge}_{12}$. We find a linear in volume dependence of $T_c(V)$ in our pressure study on $\text{LaPt}_4\text{Ge}_{12}$ and $\text{PrPt}_4\text{Ge}_{12}$, in contrast to the nonmonotonic dependence of $T_c(V)$ in the substitution series.

2. Experimental Details

The electrical resistivity and XRD experiments under hydrostatic pressure were carried out on single crystals of $\text{LaPt}_4\text{Ge}_{12}$ and $\text{PrPt}_4\text{Ge}_{12}$. The details of the sample preparation and characterization can be found in Ref. [28].

Four probe electrical-resistance measurements on $\text{LaPt}_4\text{Ge}_{12}$ and $\text{PrPt}_4\text{Ge}_{12}$ were carried out using an LR700 resistance bridge (Linear Research). Temperatures down to 1.8 K and magnetic fields up to 9 T were achieved in a Physical Property Measurement System (PPMS, Quantum Design). Pressures up to 2.74 GPa were generated in a double-layer piston-cylinder type pressure cell using silicon oil as pressure-transmitting medium [29]. The pressure dependence of the superconducting transition temperature of a piece of lead mounted along the whole sample space served as pressure gauge. The narrow superconducting transition width at all pressures confirmed the good hydrostatic pressure conditions inside the pressure cell.

The powder XRD data were obtained at the Extreme Methods of Analysis (EMA) beamline at the Brazilian Synchrotron Light Laboratory. The EMA beamline uses, as X-rays source, a 22 mm period Kyma undulator that delivers photons between 5 keV (3rd harmonic) and 30 keV (13th harmonic). The outgoing beam is monochromatized by a liquid N_2 cooled high-resolution double crystal monochromator that uses two sets of Si crystals ([111] or [311]). Finally, an achromatic set of K-B mirrors focuses the beam at the sample position with a spot size down to $1.0 \mu\text{m} \times 0.5 \mu\text{m}$ [30]. The measurements were carried out at ambient temperature using a 20 keV (9th harmonic, $\lambda = 0.6199 \text{ \AA}$) beam with a spot size of $15 \mu\text{m} \times 15 \mu\text{m}$ at the sample. The two-dimensional diffraction images were captured in a transmission geometry by a CCD MAR165 detector with pixel size of $73.2 \mu\text{m} \times 73.2 \mu\text{m}$. These images were integrated in Dioptas 0.4.0 [31]. We used the NIST (National Institute of Standards and Technology, Gaithersburg, MD, USA) standard reference material 660c (LaB_6) for calibration of detector distance and other geometrical parameters.

The single-crystalline samples were powdered and loaded each one into a diamond anvil cell (DAC) along with a ruby ball using a stainless steel gasket. The pressure was determined in situ by the wavelength of the position of the maximum of the second peak of the ruby fluorescence. We used a mixture of methanol-ethanol (4:1) as pressure transmitting

medium. The pressure was controlled by a gas-membrane mechanism that was attached to the DAC.

3. Results

The temperature dependence of the electrical resistivity (ρ) for $\text{LaPt}_4\text{Ge}_{12}$ and $\text{PrPt}_4\text{Ge}_{12}$ under various hydrostatic pressures (p) up to 2.74 GPa is shown in Figure 1a,b. For both materials $\rho(T)$ exhibits metallic behavior at all pressures, before a jump to zero resistance indicates the onset of superconductivity at low temperatures.

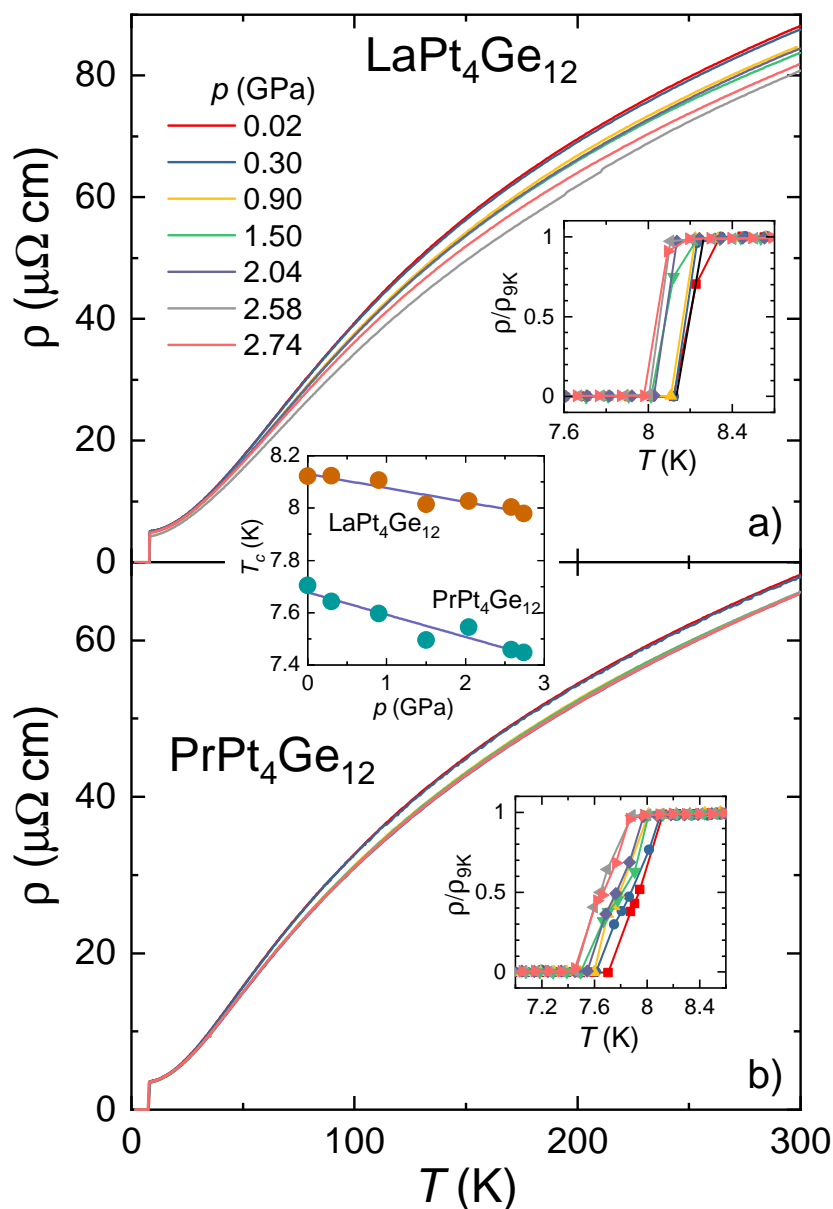


Figure 1. Electrical resistivity for (a) $\text{LaPt}_4\text{Ge}_{12}$ and (b) $\text{PrPt}_4\text{Ge}_{12}$ single crystals under various hydrostatic pressures. The corresponding insets depict the resistivity normalized by its value at 9 K. The central inset shows the pressure dependence of T_c . The lines are linear fits to the data. See text for details.

We first turn to the results on $\text{LaPt}_4\text{Ge}_{12}$. At ambient pressure, zero resistance is observed below $T_{c,\text{zero}} = 8.12$ K (inset of Figure 1a). The temperature at the midpoint of the resistive transition $T_{c,\text{mid}} = 8.24$ K agrees well with previous reports [3,9]. Increasing pressure leads to a decrease in the isothermal resistivity at room temperature ($\rho_{300\text{K}}$) up

to 2.58 GPa before it starts to increase slightly again. $T_{c,zero}(p)$ decreases only weakly with increasing pressure, by 0.14 K between ambient pressure and 2.74 GPa, the highest pressure of our investigation. Considering the scatter in the data, $T_c(p)$ can be described by a straight line, as depicted in the central inset of Figure 1. A linear fit to the data results in a slope of $dT_c(p)/dp = -53$ mK/GPa, corresponding to a normalized initial slope of $1/T_c \times dT_c/dp = d(\ln T_c)/dp = -0.0064$ GPa⁻¹. We do not observe any considerable change in the width of the superconducting transition in $\rho(T)$ in the whole pressure range.

For PrPt₄Ge₁₂, we observed $\rho = 0$ at ambient pressure below $T_{c,zero} = 7.7$ K as shown in the inset of Figure 1b. Upon increasing pressure, we find a monotonous decrease in $\rho_{300K}(p)$ in the whole investigated pressure range. $T_{c,zero}(p)$ exhibits a much stronger pressure dependence than for LaPt₄Ge₁₂. $T_{c,zero}(p)$ drops by 0.26 K from 0 to 2.74 GPa. Considering the scatter in the data, a linear fit describes the data reasonably well and gives a slope of $dT_c(p)/dp = -85$ mK/GPa and $d(\ln T_c)/dp = -0.011$ GPa⁻¹, see central inset of Figure 1. We note that Foroozani et al. reported a larger slope $dT_c(p)/dp$ obtained from an analysis of magnetic susceptibility measurements on a polycrystal [32]. Surprisingly, the normalized initial slope for PrPt₄Ge₁₂, $d(\ln T_c)/dp = -0.011$ GPa⁻¹ is almost twice as large as for LaPt₄Ge₁₂, $d(\ln T_c)/dp = -0.0064$ GPa⁻¹.

To determine the temperature dependence of the superconducting upper-critical field, $H_{c2}(T)$, we conducted measurements of $\rho(T)$ in different magnetic fields for all pressures. Representative $\rho(T)$ data are shown in the insets of Figure 2 for LaPt₄Ge₁₂ and PrPt₄Ge₁₂, respectively. The main panels display the $H_{c2}(T)$ derived from the resistivity data for selected pressures.

For LaPt₄Ge₁₂ the superconducting transition in $\rho(T)$ gradually broadens with increasing magnetic field as shown for 1.5 GPa in the inset of Figure 2a. There is almost no difference in the $H_{c2}(T)$ curves at different pressures. In the accessible temperature range above 1.8 K, $H_{c2}(T)$ exhibits an almost linear temperature dependence only a small curvature develops at high field while a small tail is observable in $H_{c2}(T)$ close to T_c . The weak tail close to T_c is consistent with multi-band superconductivity. An extrapolation of $H_{c2}(T)$ to zero temperature gives an upper threshold of $\mu_0 H_{c2}^0 \approx 1.6$ T for the upper-critical field. The pressure data are consistent with experiments on a polycrystalline sample at ambient pressure down to lower temperatures (open symbols in Figure 2a). Therefore, we may conclude that the upper-critical field, H_{c2}^0 , does not change significantly with pressure in LaPt₄Ge₁₂ in the studied pressure range.

The results of the same experiments on PrPt₄Ge₁₂ are shown in Figure 2b for selected pressures. The shape of the $H_{c2}(T)$ curves is similar as described for LaPt₄Ge₁₂ above. $H_{c2}(T)$ displays a small tail close to T_c , indicative of multi-band superconductivity, and already starts to bend over at the lowest accessible temperature. The effect of pressure on $H_{c2}(T)$ is also small, but it is more pronounced than in the case of LaPt₄Ge₁₂. An upper threshold of $\mu_0 H_{c2}^0 \approx 1.8$ T can be estimated from an extrapolation of $H_{c2}(T)$ to zero temperature. The extrapolated value agrees well with literature [33]. $\rho(T)$ data in different magnetic fields at a pressure of 0.02 and 2.74 GPa are shown in the lower and upper insets of Figure 2b, respectively. The broadening of the superconducting transition with increasing magnetic field observed in $\rho(T)$ at low pressures, here 0.02 GPa is shown, is absent at 2.74 GPa. At this pressure, the transition remains sharp up to the highest field where we can access the transition in our experimental temperature range. This is remarkable since $T_{c,zero}$, respectively, the $H_{c2}(T)$ curves are nearly unchanged by the application of pressure up to 2.74 GPa.

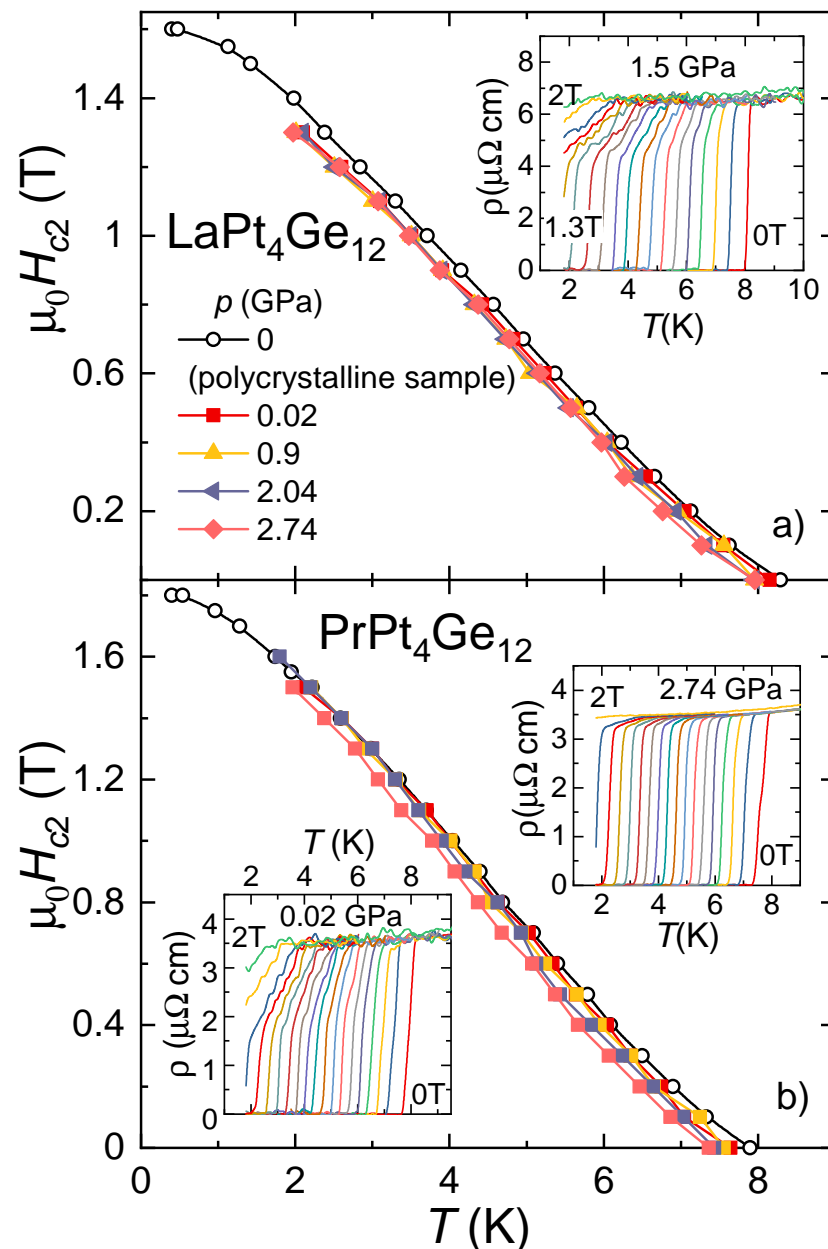


Figure 2. Magnetic field–temperature phase diagram of (a) $\text{LaPt}_4\text{Ge}_{12}$ and (b) $\text{PrPt}_4\text{Ge}_{12}$ single crystals at different pressures. The open symbols represent results of resistivity measurements at $p = 0$ on polycrystalline samples down to 350 mK using the Helium-3 option of a PPMS. The lines serve as guide to the eyes. The insets show the resistivity data in different magnetic fields for selected pressures as indicated.

Figure 3a,b shows the XRD data taken at room temperature for several pressures on $\text{LaPt}_4\text{Ge}_{12}$ and $\text{PrPt}_4\text{Ge}_{12}$, respectively. Both compounds maintain the cubic structural phase in the entire range of pressure studied up to 7.5 GPa. We can clearly identify three reflections associated with the [200], [220], and [301] planes. They are slightly shifted to higher angles upon increasing pressure, as expected due to the contraction of the crystal lattice. We used the Le-Bail method implemented in GSAS-II software package [34] to calculate the lattice parameter a as a function of pressure for both compounds. We note that here we only used the diffracted peak position to estimate the lattice parameters since the intensity and shape of the peak in our data are affected by the poor grain distribution due to small amount of sample in the DAC combined with small spot size of the beam.

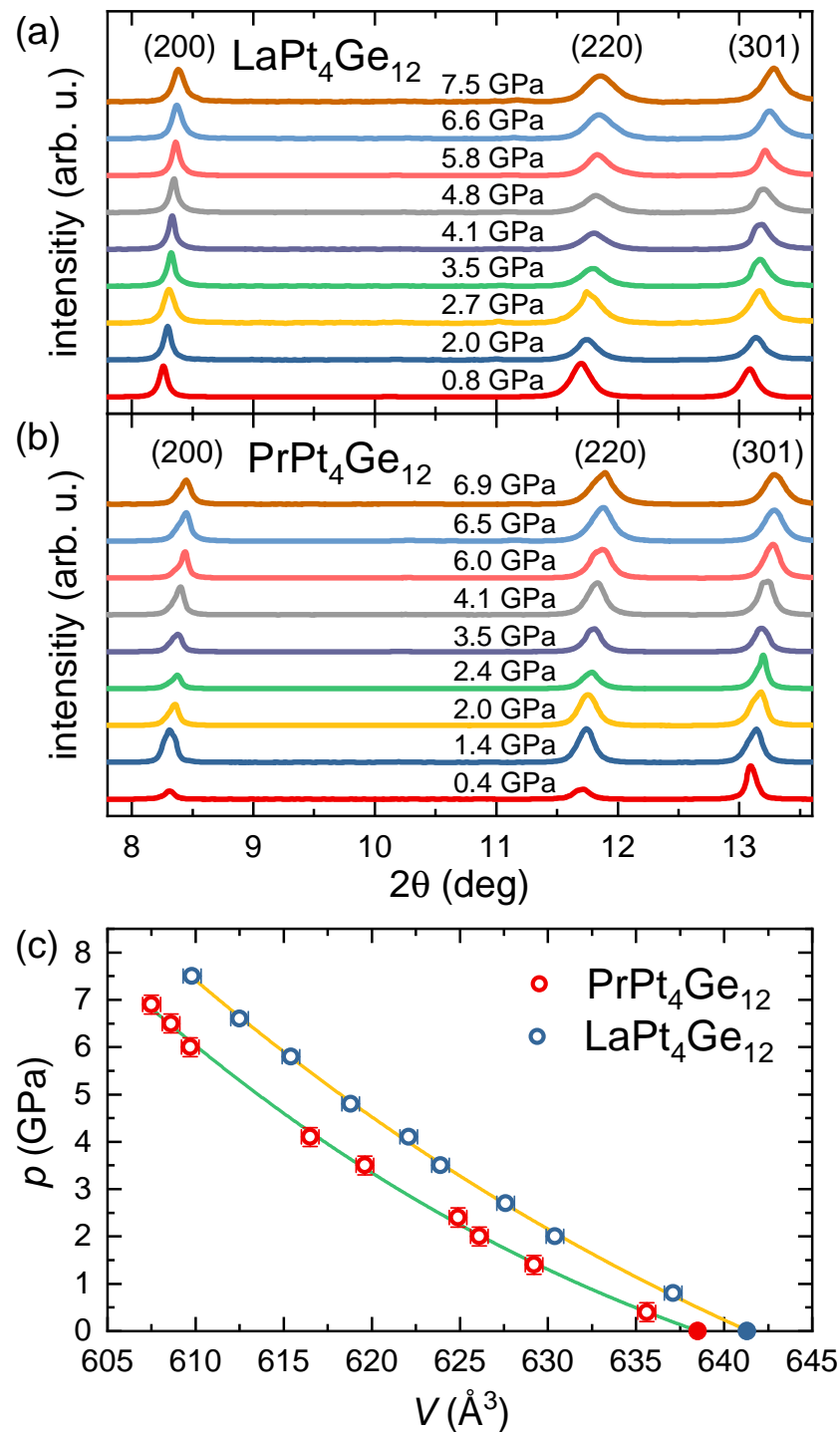


Figure 3. Normalized XRD data for different pressure values of (a) $\text{LaPt}_4\text{Ge}_{12}$ and (b) $\text{PrPt}_4\text{Ge}_{12}$ taken at room temperature. (c) Applied pressure plotted versus the unit-cell volume. The solid lines correspond to fits of the Birch-Murnaghan equation of state to the data of $\text{LaPt}_4\text{Ge}_{12}$ and $\text{PrPt}_4\text{Ge}_{12}$. The data points at $p = 0$ (solid symbols) have been taken from literature [28]. See text for details.

The pressure dependence of the unit-cell volume obtained from the experimental lattice parameters of $\text{LaPt}_4\text{Ge}_{12}$ and $\text{PrPt}_4\text{Ge}_{12}$ were fitted using the Birch-Murnaghan equation of state,

$$p(V) = \frac{3B}{2} \left[\left(\frac{V_0}{V} \right)^{\frac{7}{3}} - \left(\frac{V_0}{V} \right)^{\frac{5}{3}} \right] \left\{ 1 + \frac{3}{4}(B' - 4) \left[\left(\frac{V_0}{V} \right)^{\frac{2}{3}} - 1 \right] \right\},$$

with V_0 the unit-cell volume, the bulk modulus B and its pressure derivative B' , all at zero pressure. Figure 3c displays the results and affirms the high quality of the fits. We obtained $V_0 = (641.44 \pm 0.3) \text{ \AA}^3$ and $V_0 = (638.5 \pm 0.6) \text{ \AA}^3$ for $\text{LaPt}_4\text{Ge}_{12}$ and $\text{PrPt}_4\text{Ge}_{12}$, respectively. These values agree well with the experimental unit-cell volume at ambient pressure within the error-bars [28]. We further obtained the bulk modulus and its pressure derivative for $\text{LaPt}_4\text{Ge}_{12}$, $B_0 = (106 \pm 5) \text{ GPa}$ and $B' = (14 \pm 2)$, and for $\text{PrPt}_4\text{Ge}_{12}$, $B_0 = (83 \pm 8) \text{ GPa}$ and $B' = (23 \pm 4)$. We note that our experimental value for the bulk modulus of $\text{LaPt}_4\text{Ge}_{12}$ compares reasonably well with results from a density functional theory calculation by Tütüncü et al. [35]. There are no calculations available for $\text{PrPt}_4\text{Ge}_{12}$.

4. Discussion

Replacement of La by the smaller Pr in $\text{La}_{1-x}\text{Pr}_x\text{Pt}_4\text{Ge}_{12}$ results in a reduction of the lattice parameter a and correspondingly of the volume of the unit cell $V = a^3$ [3,12,25]. The unit-cell volume of $\text{PrPt}_4\text{Ge}_{12}$ is about 0.43% smaller than that of $\text{LaPt}_4\text{Ge}_{12}$ [28]. Therefore, in a simple picture, $\text{PrPt}_4\text{Ge}_{12}$ can be considered as a chemically pressurized analog of $\text{LaPt}_4\text{Ge}_{12}$, since the Pr-ion in $\text{PrPt}_4\text{Ge}_{12}$ is in a non-magnetic singlet crystalline electric field ground state [3,9]. In particular, no $4f$ magnetism competes with superconductivity [12]. Upon substituting Pr for La $T_c(x)$ decreases continuously up to $x \approx 0.75$, where a minimum develops before $T_c(x)$ increases again toward stoichiometric $\text{PrPt}_4\text{Ge}_{12}$ [12,25]. The nonmonotonous behavior of $T_c(x)$ and the appearance of time-reversal-breaking superconductivity in the substitution series $\text{La}_{1-x}\text{Pr}_x\text{Pt}_4\text{Ge}_{12}$ indicate that volume effects alone cannot explain the observed behavior, in particular, since substitution of La by Pr reduces the unit-cell volume linearly as function of x [12,25].

Using the results from our XRD study, we can calculate the unit-cell volume corresponding to the applied hydrostatic pressure in our electrical-transport experiments. Figure 4 presents the resulting $T - V$ phase diagram. It combines the results of our pressure study on $\text{LaPt}_4\text{Ge}_{12}$ and $\text{PrPt}_4\text{Ge}_{12}$ with literature data on the substitution series $\text{La}_{1-x}\text{Pr}_x\text{Pt}_4\text{Ge}_{12}$ [3,12,25]. We note that the structural parameters in our study as well as the ones in the studies on the substitution series were determined at room temperature. Since the thermal contraction of $\text{LaPt}_4\text{Ge}_{12}$ and $\text{PrPt}_4\text{Ge}_{12}$ is very similar this does not affect the discussion below [28]. The superconducting transition temperatures in $\text{LaPt}_4\text{Ge}_{12}$ and $\text{PrPt}_4\text{Ge}_{12}$ depend in a simple linear relation on the unit-cell volume. From fits to the data, we obtain comparable slopes of $dT_c(V)/dV = -11.93 \text{ mK}/\text{\AA}^3$ and $dT_c(V)/dV = -15.65 \text{ mK}/\text{\AA}^3$ for $\text{LaPt}_4\text{Ge}_{12}$ and $\text{PrPt}_4\text{Ge}_{12}$, respectively (see Figure 4). We note that due to the different bulk moduli of the two materials, the difference in $dT_c(V)/dV$ between $\text{LaPt}_4\text{Ge}_{12}$ and $\text{PrPt}_4\text{Ge}_{12}$ appears to be considerably smaller than the difference in the pressure dependence $dT_c(p)/dp$. In contrast to the simple linear and weak dependence of T_c on the unit-cell volume in $\text{LaPt}_4\text{Ge}_{12}$ and $\text{PrPt}_4\text{Ge}_{12}$, $T_c(V)$ display a much stronger and non-monotonous volume dependence in the substitution series $\text{La}_{1-x}\text{Pr}_x\text{Pt}_4\text{Ge}_{12}$, as can be seen in Figure 4.

Fermi-surface studies on $\text{LaPt}_4\text{Ge}_{12}$ and $\text{PrPt}_4\text{Ge}_{12}$ find that their electronic band structures are nearly identical with moderately enhanced effective masses for the six bands crossing at the Fermi energy [22]. These findings are in line with phonon mediated Cooper pairing and consistent with multi-gap superconductivity in both compounds [22]. A phonon mediated superconducting coupling mechanism has been indeed suggested for $\text{LaPt}_4\text{Ge}_{12}$ [35]. It is therefore not surprising that T_c exhibits the same dependence on V in $\text{LaPt}_4\text{Ge}_{12}$ and $\text{PrPt}_4\text{Ge}_{12}$. The similarities in the band structure are further in agreement with the continuous evolution of T_c in the substitution series. However, $T_c(V)$ in the substitution series $\text{La}_{1-x}\text{Pr}_x\text{Pt}_4\text{Ge}_{12}$ displays a non-monotonous behavior with a pronounced minimum. Furthermore, there is evidence for time-reversal-symmetry breaking superconductivity in the substitution series, which is absent on the La-rich side [25]. We may therefore speculate that in $\text{LaPt}_4\text{Ge}_{12}$ and $\text{PrPt}_4\text{Ge}_{12}$, application of pressure in the investigated pressure range leads to a rigid shift of the band structure, similar to the findings in $\text{BaPt}_{4-x}\text{Au}_x\text{Ge}_{12}$, where a linear change in $T_c(V)$ has been observed before and

related to a rigid shift of the electronic band structure [36,37]. In contrast, Pr substitution in $\text{La}_{1-x}\text{Pr}_x\text{Pt}_4\text{Ge}_{12}$ generates distinct changes in the multi-band nature of the superconductivity, which goes beyond this simple picture and deserves further investigations.

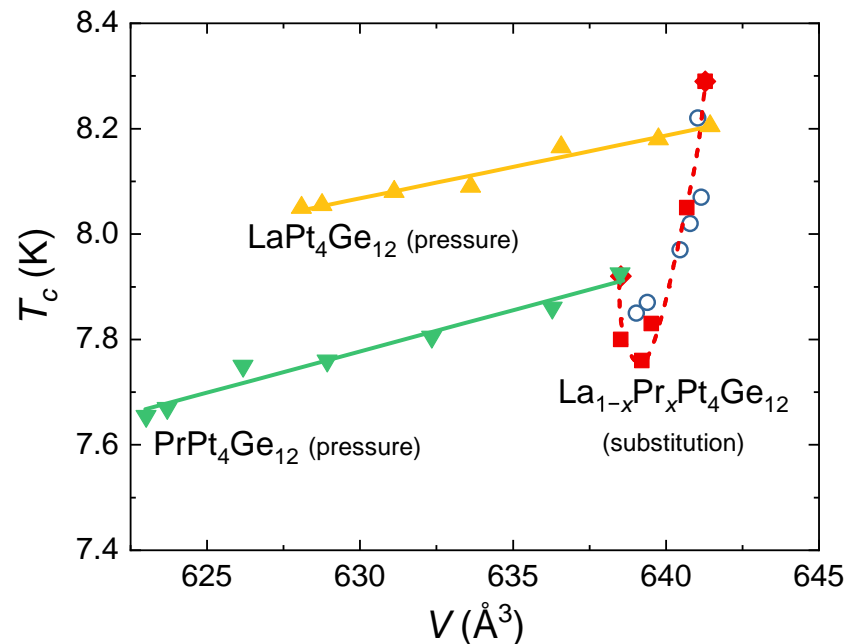


Figure 4. Superconducting temperature—unit-cell volume phase diagram of pressurized $\text{LaPt}_4\text{Ge}_{12}$ and $\text{PrPt}_4\text{Ge}_{12}$ combined with data of the substitution series $\text{La}_{1-x}\text{Pr}_x\text{Pt}_4\text{Ge}_{12}$. The open blue symbols correspond to data determined from specific heat [25], while the solid red diamonds [3] and the solid red squares [12] represent our previously published data based on magnetic susceptibility measurements taken in a magnetic field of $\mu_0 H = 2$ mT. The straight lines are fits to the data and the red dashed line is a guide to the eye.

5. Summary and Conclusions

We carried out electrical resistivity and X-ray diffraction experiments under hydrostatic pressures on the two skutterudite compounds, $\text{LaPt}_4\text{Ge}_{12}$ and $\text{PrPt}_4\text{Ge}_{12}$. We find a pressure-induced linear suppression of the superconduction transition temperature in both materials. Based on our XRD data, we derive a bulk modulus of 106 GPa for $\text{LaPt}_4\text{Ge}_{12}$ and 83 GPa for $\text{PrPt}_4\text{Ge}_{12}$. With the help of the bulk modulus, we established a superconducting temperature—unit-cell volume phase diagram by combining the pressure data on $\text{LaPt}_4\text{Ge}_{12}$ and $\text{PrPt}_4\text{Ge}_{12}$ with results from the substitution series $\text{La}_{1-x}\text{Pr}_x\text{Pt}_4\text{Ge}_{12}$. The comparison of the effect of hydrostatic pressure on $\text{LaPt}_4\text{Ge}_{12}$ and $\text{PrPt}_4\text{Ge}_{12}$ with that of chemical substitution indicates marked differences. While the weak linear dependence of T_c on the unit-cell volume with almost the same slopes for both compounds can be explained in a simple picture consistent with phonon mediated superconductivity, the nonmonotonous dependence of $T_c(x)$ in $\text{La}_{1-x}\text{Pr}_x\text{Pt}_4\text{Ge}_{12}$ suggests more complex competing behaviors in the substitution series, which stimulate further detailed investigations.

Author Contributions: Conceptualization, M.N.; sample preparation R.G. and A.L.-J.; investigation, G.A.L., K.M. and W.S.; data analysis, G.A.L., K.M., R.D.d.R. and M.N.; writing—original draft, M.N.; writing—review & editing, G.A.L., K.M., R.G., A.L.-J., R.D.d.R., W.S. and M.N. All authors have read and agreed to the published version of the manuscript.

Funding: R.D.d.R. acknowledges financial support from the Brazilian agencies CNPq and FAPESP (Grant 2018/00823-0) and from the Max Planck Society under the auspices of the Max Planck Partner Group R. D. dos Reis of the MPI for Chemical Physics of Solids, Dresden, Germany.

Data Availability Statement: The data presented in this study are available on reasonable request from the corresponding author.

Acknowledgments: This research used facilities of the Brazilian Synchrotron Light Laboratory (LNLS), part of the Brazilian Centre for Research in Energy and Materials (CNPEM), a private non-profit organization under the supervision of the Brazilian Ministry for Science, Technology, and Innovations (MCTI). The EMA beamline staff is acknowledged for the assistance during the experiments with proposal number 20210180.

Conflicts of Interest: The authors declare no conflict of interest.

References

1. Jeitschko, W.; Braun, D. LaFe₄P₁₂ with filled CoAs₃-type structure and isotypic lanthanoid-transition metal polyphosphides. *Acta Crystallogr. B* **1977**, *33*, 3401–3406. [[CrossRef](#)]
2. Bauer, E.; Grytsiv, A.; Chen, X.Q.; Melnychenko-Koblyuk, N.; Hilscher, G.; Kaldarar, H.; Michor, H.; Royanian, E.; Giester, G.; Rotter, M.; et al. Superconductivity in novel Ge-based skutterudites: Sr,BaPt₄Ge₁₂. *Phys. Rev. Lett.* **2007**, *99*, 217001. [[CrossRef](#)]
3. Gumeniuk, R.; Schnelle, W.; Rosner, H.; Nicklas, M.; Leithe-Jasper, A.; Grin, Y. Superconductivity in the platinum germanides MPt₄Ge₁₂ (M = rare-earth or alkaline-earth metal) with filled skutterudite structure. *Phys. Rev. Lett.* **2008**, *100*, 017002. [[CrossRef](#)]
4. Kaczorowski, D.; Tran, V.H. Superconductivity in the actinoid-bearing filled skutterudite ThPt₄Ge₁₂. *Phys. Rev. B* **2008**, *77*, 180504R. [[CrossRef](#)]
5. Bauer, E.; Chen, X.Q.; Rogl, P.; Hilscher, G.; Michor, H.; Royanian, E.; Podloucky, R.; Giester, G.; Sologub, O.; Goncalves, A.P. Superconductivity and spin fluctuations in {Th,U}Pt₄Ge₁₂ skutterudites. *Phys. Rev. B* **2008**, *78*, 064516. [[CrossRef](#)]
6. Nicklas, M.; Gumeniuk, R.; Schnelle, W.; Rosner, H.; Leithe-Jasper, A.; Steglich, F.; Grin, Y. Magnetic order in the filled skutterudites RPt₄Ge₁₂ (R = Nd, Eu). *J. Phys. Conf. Ser.* **2011**, *273*, 012118. [[CrossRef](#)]
7. Gumeniuk, R.; Schoneich, M.; Leithe-Jasper, A.; Schnelle, W.; Nicklas, M.; Rosner, H.; Ormeci, A.; Burkhardt, U.; Schmidt, M.; Schwarz, U.; et al. High-pressure synthesis and exotic heavy-fermion behaviour of the filled skutterudite SmPt₄Ge₁₂. *New J. Phys.* **2010**, *12*, 103035. [[CrossRef](#)]
8. Baenitz, M.; Sarkar, R.; Gumeniuk, R.; Leithe-Jasper, A.; Schnelle, W.; Rosner, H.; Burkhardt, U.; Schmidt, M.; Schwarz, U.; Kaczorowski, D.; et al. Ge-based skutterudites MPt₄Ge₁₂: A comparative Pt-195 NMR study. *Phys. Status Solidi B* **2010**, *247*, 740–742. [[CrossRef](#)]
9. Toda, M.; Sugawara, H.; Magishi, K.; Saito, T.; Koyama, K.; Aoki, Y.; Sato, H. Electrical, Magnetic and NMR Studies of Ge-Based Filled Skutterudites RPt₄Ge₁₂ (R = La, Ce, Pr, Nd). *J. Phys. Soc. Jpn.* **2008**, *77*, 124702. [[CrossRef](#)]
10. Nicklas, M.; Kirchner, S.; Borth, R.; Gumeniuk, R.; Schnelle, W.; Rosner, H.; Borrmann, H.; Leithe-Jasper, A.; Grin, Y.; Steglich, F. Charge-Doping-Driven Evolution of Magnetism and Non-Fermi-Liquid Behavior in the Filled Skutterudite CePt₄Ge_{12-x}Sb_x. *Phys. Rev. Lett.* **2012**, *109*, 236405. [[CrossRef](#)]
11. Galera, R.M.; Opagiste, C.; Amara, M.; Zbiri, M.; Rols, S. First neutron studies of the magnetism and rattling modes in CePt₄Ge₁₂. *J. Phys. Conf. Ser.* **2015**, *592*, 012011. [[CrossRef](#)]
12. Maisuradze, A.; Schnelle, W.; Khasanov, R.; Gumeniuk, R.; Nicklas, M.; Rosner, H.; Leithe-Jasper, A.; Grin, Y.; Amato, A.; Thalmeier, P. Evidence for time-reversal symmetry breaking in superconducting PrPt₄Ge₁₂. *Phys. Rev. B* **2010**, *82*, 024524. [[CrossRef](#)]
13. Kanetake, F.; Mukuda, H.; Kitaoka, Y.; Magishi, K.; Sugawara, H.; Itoh, K.M.; Haller, E.E. Superconducting Characteristics of Filled Skutterudites LaPt₄Ge₁₂ and PrPt₄Ge₁₂: Ge-73-NQR/NMR Studies. *J. Phys. Soc. Jpn.* **2010**, *79*, 063702. [[CrossRef](#)]
14. Zhang, J.L.; Chen, Y.; Jiao, L.; Gumeniuk, R.; Nicklas, M.; Chen, Y.H.; Yang, L.; Fu, B.H.; Schnelle, W.; Rosner, H.; et al. Multiband superconductivity in PrPt₄Ge₁₂ single crystals. *Phys. Rev. B* **2013**, *87*, 064502. [[CrossRef](#)]
15. Nakamura, Y.; Okazaki, H.; Yoshida, R.; Wakita, T.; Takeya, H.; Hirata, K.; Hirai, M.; Muraoka, Y.; Yokoya, T. Comparative photoemission studies on the superconducting gap of the filled skutterudite superconductors LaPt₄Ge₁₂ and PrPt₄Ge₁₂. *Phys. Rev. B* **2012**, *86*, 014521. [[CrossRef](#)]
16. Chandra, L.S.S.; Chattopadhyay, M.K.; Roy, S.B. Critical current density and vortex pinning in the two gap superconductor PrPt₄Ge₁₂. *Supercond. Sci. Technol.* **2012**, *25*, 105009. [[CrossRef](#)]
17. Chandra, L.S.S.; Chattopadhyay, M.K.; Roy, S.B. Evidence for two superconducting gaps in the unconventional superconductor PrPt₄Ge₁₂. *Philos. Mag.* **2012**, *92*, 3866–3881. [[CrossRef](#)]
18. Huang, K.; Shu, L.; Lum, I.K.; White, B.D.; Janoschek, M.; Yazici, D.; Hamlin, J.J.; Zocco, D.A.; Ho, P.C.; Baumbach, R.E.; et al. Probing the superconductivity of PrPt₄Ge₁₂ through Ce substitution. *Phys. Rev. B* **2014**, *89*, 035145. [[CrossRef](#)]
19. Huang, K.; Yazici, D.; White, B.D.; Jeon, I.; Breindel, A.J.; Pouse, N.; Maple, M.B. Superconducting and normal state properties of the systems La_{1-x}M_xPt₄Ge₁₂ (M = Ce, Th). *Phys. Rev. B* **2016**, *94*, 094501. [[CrossRef](#)]
20. Chandra, L.S.S.; Chattopadhyay, M.K.; Roy, S.B.; Pandey, S.K. Thermal properties and electronic structure of superconducting germanide skutterudites LaPt₄Ge₁₂ and PrPt₄Ge₁₂: A multi-band perspective. *Philos. Mag.* **2016**, *96*, 2161–2175. [[CrossRef](#)]
21. Singh, Y.P.; Adhikari, R.B.; Zhang, S.; Huang, K.; Yazici, D.; Jeon, I.; Maple, M.B.; Dzero, M.; Almasan, C.C. Multiband superconductivity in the correlated electron filled skutterudite system Pr_{1-x}Ce_xPt₄Ge₁₂. *Phys. Rev. B* **2016**, *94*, 144502. [[CrossRef](#)]
22. Bergk, B.; Klotz, J.; Forster, T.; Gumeniuk, R.; Leithe-Jasper, A.; Lorenz, V.; Schnelle, W.; Nicklas, M.; Rosner, H.; Grin, Y.; et al. Fermi surface studies of the skutterudite superconductors LaPt₄Ge₁₂ and PrPt₄Ge₁₂. *Phys. Rev. B* **2019**, *99*, 245115. [[CrossRef](#)]

23. Zhang, J.; MacLaughlin, D.E.; Hillier, A.D.; Ding, Z.F.; Huang, K.; Maple, M.B.; Shu, L. Broken time-reversal symmetry in superconducting $\text{Pr}_{1-x}\text{Ce}_x\text{Pt}_4\text{Ge}_{12}$. *Phys. Rev. B* **2015**, *91*, 104523. [[CrossRef](#)]
24. Zang, J.W.; Zhang, J.; Zhu, Z.H.; Ding, Z.F.; Huang, K.; Peng, X.R.; Hillier, A.D.; Shu, L. Broken Time-Reversal Symmetry in Superconducting Partially Filled Skutterudite $\text{Pr}_{1-\text{delta}}\text{Pt}_4\text{Ge}_{12}$. *Chin. Phys. Lett.* **2019**, *36*, 107402. [[CrossRef](#)]
25. Zhang, J.; Ding, Z.F.; Huang, K.; Tan, C.; Hillier, A.D.; Biswas, P.K.; MacLaughlin, D.E.; Shu, L. Broken time-reversal symmetry in superconducting $\text{Pr}_{1-x}\text{La}_x\text{Pt}_4\text{Ge}_{12}$. *Phys. Rev. B* **2019**, *100*, 024508. [[CrossRef](#)]
26. Pfau, H.; Nicklas, M.; Stockert, U.; Gumeniuk, R.; Schnelle, W.; Leithe-Jasper, A.; Grin, Y.; Steglich, F. Superconducting gap structure of the skutterudite $\text{LaPt}_4\text{Ge}_{12}$ probed by specific heat and thermal transport. *Phys. Rev. B* **2016**, *94*, 054523. [[CrossRef](#)]
27. Zhang, J.L.; Pang, G.M.; Jiao, L.; Nicklas, M.; Chen, Y.; Weng, Z.F.; Smidman, M.; Schnelle, W.; Leithe-Jasper, A.; Maisuradze, A.; et al. Weak interband-coupling superconductivity in the filled skutterudite $\text{LaPt}_4\text{Ge}_{12}$. *Phys. Rev. B* **2015**, *92*, 220503. [[CrossRef](#)]
28. Gumeniuk, R.; Borrmann, H.; Ormeci, A.; Rosner, H.; Schnelle, W.; Nicklas, M.; Grin, Y.; Leithe-Jasper, A. Filled platinum germanium skutterudites $\text{MPt}_4\text{Ge}_{12}$ (M = Sr, Ba, La-Nd, Sm, Eu): Crystal structure and chemical bonding. *Z. Kristallogr.* **2010**, *225*, 531–543. [[CrossRef](#)]
29. Nicklas, M. Pressure Probes. In *Strongly Correlated Systems: Experimental Techniques*; Avella, A., Mancini, F., Eds.; Springer: Berlin/Heidelberg, Germany, 2015; pp. 173–204. [[CrossRef](#)]
30. dos Reis, R.D.; Kaneko, U.F.; Francisco, B.A.; Fonseca, J., Jr.; Eleoterio, M.A.S.; Souza-Neto, N.M. Preliminary Overview of the Extreme Condition Beamline (EMA) at the new Brazilian Synchrotron Source (Sirius). *J. Phys. Conf. Ser.* **2020**, *1609*, 012015. [[CrossRef](#)]
31. Prescher, C.; Prakapenka, V.B. DIOPTAS: A program for reduction of two-dimensional X-ray diffraction data and data exploration. *High Press. Res.* **2015**, *35*, 223–230. [[CrossRef](#)]
32. Foroozani, N.; Hamlin, J.J.; Schilling, J.S.; Baumbach, R.E.; Lum, I.K.; Shu, L.; Huang, K.; Maple, M.B. Dependence of the superconducting transition temperature of the filled skutterudite compound $\text{PrPt}_4\text{Ge}_{12}$ on hydrostatic pressure. *Phys. C Supercond.* **2013**, *485*, 160–162. [[CrossRef](#)]
33. Maisuradze, A.; Nicklas, M.; Gumeniuk, R.; Baines, C.; Schnelle, W.; Rosner, H.; Leithe-Jasper, A.; Grin, Y.; Khasanov, R. Superfluid Density and Energy Gap Function of Superconducting $\text{PrPt}_4\text{Ge}_{12}$. *Phys. Rev. Lett.* **2009**, *103*, 147002. [[CrossRef](#)] [[PubMed](#)]
34. Toby, B.H. GSAS-II: The genesis of a modern open-source all purpose crystallography software package. *J. Appl. Cryst.* **2013**, *46*, 544–549. [[CrossRef](#)]
35. Tütüncü, H.M.; Karaca, E.; Srivastava, G.P. Electron-phonon superconductivity in the filled skutterudites $\text{LaRu}_4\text{P}_{12}$, $\text{LaRu}_4\text{As}_{12}$, and $\text{LaPt}_4\text{Ge}_{12}$. *Phys. Rev. B* **2017**, *95*, 214514. [[CrossRef](#)]
36. Gumeniuk, R.; Rosner, H.; Schnelle, W.; Nicklas, M.; Leithe-Jasper, A.; Grin, Y. Optimization of the superconducting transition temperature of the filled skutterudite $\text{BaPt}_4\text{Ge}_{12}$ by gold substitution. *Phys. Rev. B* **2008**, *78*, 052504. [[CrossRef](#)]
37. Maisuradze, A.; Gumeniuk, R.; Schnelle, W.; Nicklas, M.; Baines, C.; Khasanov, R.; Amato, A.; Leithe-Jasper, A. Superconducting parameters of $\text{BaPt}_{4-x}\text{Au}_x\text{Ge}_{12}$ filled skutterudite. *Phys. Rev. B* **2012**, *86*, 174513. [[CrossRef](#)]